Hydrol. Earth Syst. Sci. Discuss., doi:10.5194/hess-2016-661, 2017
Manuscript under review for journal Hydrol. Earth Syst. Sci.
Published: 10 January 2017

Hydrology and Earth System Sciences
Open Access
EGU
Discussions

Effects of multi-temporal high-resolution remote sensing products on simulated hydrometeorological variables in a cultivated area (southwestern France)

Jordi Etchanchu[1], Vincent Rivalland[1], Simon Gascoin[1], Jérôme Cros[1], Aurore Brut[1], Gilles Boulet[1]

[1] *CESBIO, Université de Toulouse, CNES, CNRS, IRD, UPS, Toulouse, France*

Correspondence to: Jordi Etchanchu (jordi.etchanchu@cesbio.cnes.fr)

Abstract. Agricultural landscapes often include a patchwork of crop fields whose seasonal evolution is dependent on specific crop rotation patterns and phenologies. This temporal and spatial heterogeneity affects surface hydrometeorological processes as simulated by land surface and distributed hydrological models. Sentinel-2 mission satellite remote sensing products allow for the monitoring of land cover and vegetation dynamics at unprecedented spatial resolutions and revisit frequencies (20 m and 5 days, respectively) that are fully compatible with such heterogeneous agricultural landscapes. Here, we evaluate the impact of Sentinel-2-like remote sensing data on the simulation of surface water and energy flux via the ISBA-SURFEX land surface model. The study area is a 24 km by 24 km agricultural zone in southwestern France. An initial reference simulation was conducted from 2006-2010 using the ECOCLIMAP-II database. This global numerical land ecosystem database was created at a 1 km resolution and includes an ecosystem classification with a consistent set of land surface parameters required for the model, such as the Leaf Area Index (LAI) and albedo measures. The LAI of ECOCLIMAP is climatologic and derived from a 2000-2005 analysis of MODIS satellite products. This low resolution induces that several vegetation covers can be mixed in a model cell. The climatic construction of LAI dynamics also suggests that there is no interannual variability in the vegetation cycle. A second simulation was performed by forcing the same model with annual land cover maps and monthly LAI values derived from a series of 105 8 m-resolution Formosat-2 images for the same period. Both simulations were conducted at the parcel scale, i.e., a computation unit covers an area of connected pixels of the same vegetation type (a crop field, forest patch, etc.). To evaluate our simulations, we used in situ measurements of evapotranspiration and latent and sensible heat flux from two eddy covariance stations in the study area. Our results show that the use of Formosat-2 high-resolution products significantly improves simulated evapotranspiration results with respect to ECOCLIMAP-II, especially when a surface is covered with summer crops (the correlation coefficient with monthly measurements is increased by roughly 0.3 and the root mean square error is decreased by roughly 31%). This finding is attributable to a better description of LAI evolution processes reflected by Formosat-2 data, which further modify soil water content and drainage levels of deep soil reservoirs. Effects on annual drainage patterns remain small but significant, i.e., an increase roughly equivalent to 4% of annual precipitation levels from Formosat-2 data in comparison to reference values. In smaller proportions, runoff is also increased by roughly 1% of annual precipitation when using

Hydrol. Earth Syst. Sci. Discuss., doi:10.5194/hess-2016-661, 2017
Manuscript under review for journal Hydrol. Earth Syst. Sci.
Published: 10 January 2017

Hydrology and Earth System Sciences
Discussions

Formosat-2 data. This study illustrates the potential for the Sentinel-2 mission to better represent effects of crop management on water budgeting for large, anthropized river basins.

1 Introduction

In a heavily anthropized river basin, agricultural practices modify the type and evolution of vegetation cover present, which can profoundly alter hydrological cycles. In such basins, the more accurate description of crop dynamics and of their effects on water flux is critical to improving the monitoring of water resources (Foley & al., 2005; Martin & al. 2016).

Land surface models (LSMs), such as the Variable Infiltration Capacity or SURFEX models, are increasingly used as distributed hydrological models to study and forecast water resource evolution (e.g., Habets & al., 2008; Tesemma & al., 2015). In land surface models or Soil-Vegetation Atmosphere Transfer schemes (SVAT), the Leaf Area Index (LAI), which represents the evaporative surface area of vegetation, is the main index used to parameterize the effect of vegetation dynamics on evapotranspiration. The LAI is often derived or directly taken from reference tables organized by vegetation type (Verseghy & al., 1993; Maurer & al., 2002; Masson & al., 2003; Oleson & al., 2008; Boussetta & al., 2013; Faroux & al., 2013). The LAI is generally computed from low- to mid-resolution long-term satellite records from AVHRR or MODIS, but it is climatological (interannually invariant), i.e., it does not allow one to determine the impact of annual vegetation variability on water and energy flux on the land surface (Tang & al., 2012; Ford & Quiring, 2013). Studies have shown that prescribing an annual variable of remotely sensed the LAI in LSM improves estimations of water and energy flux between the soil and atmosphere, and mainly through evapotranspiration (Van den Hurk & al., 2003; Jarlan & al., 2008; Tang & al., 2012; Ford & Quiring, 2013). These studies used LAI values drawn from low- to mid-resolution satellite imagery, i.e., AVHRR (Van den Hurk & al., 2003) or MODIS (Tang & al., 2012; Ford & Quiring, 2013). However, for many cultivated areas, field plot areas rarely exceed typical MODIS product pixel sizes (500 m, i.e., 25 hectares). As a result, MODIS pixels contain mixed LAI signatures of different crop types. Trezza & al. (2013) and Nagler & al. (2013) concluded that the use of remote sensing products with a 500 m spatial resolution (in their cases, the MODIS Normalized Difference Vegetation Index) generates inaccurate evapotranspiration estimations. Indeed spatially averaging vegetation indexes such as the LAI also involves averaging different types of vegetation with different phenologies, degrading their actual temporal variability. This can be exacerbated for regions where both summer and winter crops are cultivated, as is the case for our study area in southwestern France.

The recently launched Sentinel-2 mission will generate multispectral imagery of land areas at a decametric resolution (10 m to 60 m depending on the band) over a 5-day revisit period. These data can improve descriptions of vegetation and water processes in agricultural landscapes for which mid-resolution imagery has not been adapted (Ferrant & al., 2014; Ferrant & al., 2016).

In this study, we used the ISBA land surface model as part of the SURFEX modeling platform (Masson & al., 2013). The SURFEX was developed to represent surface processes of the operational atmospheric models and hydrological models of

Hydrol. Earth Syst. Sci. Discuss., doi:10.5194/hess-2016-661, 2017
Manuscript under review for journal Hydrol. Earth Syst. Sci.
Published: 10 January 2017

Météo-France. It is also used for research purposes in the fields of climatology, meteorology and hydrology. The ISBA is a submodel that simulates water and energy exchange in the soil-vegetation-atmosphere continuum (outside of urban and lake areas). It uses the ECOCLIMAP-II database to determine vegetation types and associated parameters (e.g., LAI, fractional vegetation cover, and albedo) at a spatial resolution of 1 km (Masson & al., 2003; Faroux & al., 2013). The ECOCLIMAP-II LAI is climatological with a temporal resolution of 10 days. It was derived from MODIS and SPOT-VEGETATION satellite observations collected between 1999 and 2005. Up to 12 vegetation types or plant functional types (PFTs) can be included in an ECOCLIMAP-II grid cell. The LAI of each PFT is determined by unmixing the grid cell MODIS LAI using neighboring, unmixed pixels.

This study evaluates the impact of introducing high-resolution information on vegetation type and the LAI from Sentinel-2-like observations rather than ECOCLIMAP-II in ISBA-SURFEX simulations. The study area is a pilot site in southwestern France (Dejoux & al., 2012). This site is considered to be representative of the cultivated area in the upper Garonne River Basin. A fraction (estimated at 13%) of crop fields in the area is irrigated, but we chose not to focus on effects of irrigation due to a lack of spatially distributed data on irrigation quantity and timing. LAI and land cover values were determined from a 5-year time series of Formosat-2 satellite images, which has similar spatio-temporal characteristics as Sentinel-2. The model was applied at the "field" scale to identify a homogeneous vegetation type for each computation unit (one computation unit has only one PFT). This field-scale modeling approach allows one to determine the spatial variability of LAI values between fields while limiting the computation time in comparison to a pixel-based approach. Our results are compared to in situ measurements of evapotranspiration and sensible heat flux and to a reference simulation based on ECOCLIMAP-II. Finally, we discuss the limitations of this work and challenges that must be addressed when upscaling this study to the Garonne River Basin scale using Sentinel-2 data.

2 Model and data

2.1 SURFEX-ISBA model and forcing

SURFEX is a modeling platform developed by the CNRM/Meteo-France to simulate exchanges between land surfaces and the atmosphere (Masson & al., 2013). It is composed of four modules to simulate radiative budget and hydrological flux patterns for towns, lakes, oceans and natural areas. In this study, we used the ISBA nature model. The ISBA model uses meteorological and physiographic data to simulate energy and water flux between land surfaces and the atmosphere (Fig. 1). The meteorological forcing is drawn from SAFRAN reanalysis data (Quintana & al., 2007), which provides precipitation data (in solid and liquid form), air temperature and specific humidity data at 2 meters, air pressure data, and wind and solar radiation data at hourly time intervals at an 8 km resolution. The SAFRAN data were spatially linearly interpolated to match parcel centroïds. Regarding soil parameters, by default, the ISBA uses the Harmonized World Soil Database (FAO/IIASA/ISRIC/ISS-CAS/JRC, 2012), which gives the percentage of clay and sand at a 30 arc-second (~1 km) resolution. Soil parameters were then computed using empirical pedotransfer functions (Masson & al., 2013).

Hydrol. Earth Syst. Sci. Discuss., doi:10.5194/hess-2016-661, 2017
Manuscript under review for journal Hydrol. Earth Syst. Sci.
Published: 10 January 2017

The ECOCLIMAP-II database (Faroux & al., 2013) is used to describe vegetation cover at a 1 km resolution, thus corresponding to the resolution of the SURFEX-ISBA simulation grid. Vegetation parameters were deduced from satellite products (MODIS, SPOT, FORMOSAT, etc.) for 273 ecosystems. These ecosystems were based on vegetation types, climates and soil textures. Twelve different functional plant types (PFT, also referred to as patches) are considered in the ISBA (Fig. 2) to describe these ecosystems. Each pixel in the SURFEX-ISBA belongs to a unique ecosystem and thus is described as a combination of these patches. Vegetation parameters are thus determined for each ecosystem patch. Some of the parameters are fixed such as root depth and minimal stomatal resistance, and some are temporally variable such as albedo and the LAI. In particular, the LAI follows a cycle determined from MODIS LAI analysis data for 2000 to 2005 averaged for each vegetation type of each ecosystem with a temporal resolution of 10 days (Faroux & al., 2013).

The ISBA then uses these parameters to simulate fluxes at a 1 km resolution. The SURFEX separately simulates all variables for each vegetation type present in the pixels, and then based on the fraction of each type as a weighting coefficient, it calculates global pixel fluxes.

2.2 Data

All remote sensing and in situ data were collected as part of the Observatoire Spatial Régional (OSR) project for an agricultural area of southwestern France near Toulouse (Fig. 3, Dejoux & al., 2012). This area is considered to be representative of the cultivated area of the Garonne River Basin, which is characterized by a variety of land cover forms. The two main types of crops found in this area are irrigated summer crops such as maize or soy plants and non-irrigated rotation crops such as wheat and sunflower plants.

2.2.1 Formosat-2 Leaf Area Index

Formosat-2 is an NSPO (Taiwan) satellite that can generate daily multispectral images of the Earth's surface at an 8 m resolution and with a swath of 24 km. It functions on a tasking mode, i.e., it does not acquire data systematically like Sentinel-2 but rather must be programmed for a target area. Its sensor detects radiation within four frequency bands of blue, green, red and near-infrared. After geometric, atmospheric and radiometric corrections were made and clouds are detected (Hagolle & al., 2008 and 2010), measured reflectances were entered into the neural network BV-NET, which inverts the PROSAIL radiative transfer model (Claverie, 2012). This neural network deduces a set of vegetation parameters (among them the LAI and fraction of vegetation cover (FCOVER)) for each pixel. It thus generates 8-m resolution LAI maps for each date and pixels without cloud obstruction. Finally, we had access to 105 clear images on our study area for 2006-2010. The LAI product was validated by Veloso & al. (2012) for the same area and time period as those used in this study with destructive measurements on the vegetation. The time series of LAI maps was then spatially averaged at the field scale using the land cover map (Sect. 2.2.2 below), was interpolated between available dates and was finally temporally averaged to obtain monthly forcings of LAI for each field of the domain.

Hydrol. Earth Syst. Sci. Discuss., doi:10.5194/hess-2016-661, 2017
Manuscript under review for journal Hydrol. Earth Syst. Sci.
Published: 10 January 2017

2.2.2 Formosat-2 land cover maps

Annual land cover maps were generated using the previously described Formosat-2 image time series (Fig. 4, Ducrot & al., 2005, 2007 and 2009). Then, a supervised classification algorithm was applied to determine the vegetation type of each parcel. The algorithm uses annual Normalized Difference Vegetation Index (NDVI) profiles to separate pixels into classes with similar NDVI profiles. We identified 34 classes. The classification was adjusted through "Politique Agricole Commune" observations, which assign crop types for a subset of fields in images from farmers' official declarations.

2.2.3 In situ measurements

We used in situ measurements drawn from two eddy covariance stations in the simulation domain located at Auradé (43°32'58.81" N, 01°06'22.08" E) and Lamasquère (43°50'05" N, 01°24'19" E) to evaluate the simulations. The Auradé plot is located on a hillside near Garonne river terraces. It belongs to a private cereal production farm with a wheat-sunflower-wheat-rapeseed rotation. At this site, only grain is exported, straw is stored and the plot is never irrigated. The Lamasquère plot is part of an experimental milk production farm. It is positioned along the Touch River and is characterized by a maize-winter wheat-maize-winter wheat rotation. All aboveground biomass is exported as cow feed and bedding. Maize grown in the Lamasquère plot is irrigated. In 2006, irrigation levels were measured at 147 mm between June and August.

Each flux site is equipped with 1) eddy covariance systems to measure half-hourly sensible heat flux and evapotranspiration; 2) meteorological sensors that measure radiation (CNR1, Kipp & Zonen), wind speed (Windvane / prop Young), air temperature and humidity (HMP35, Vaisala); and 3) soil profile probes for water content measurements (CS616, Campbell Scientific) collected at depths of 5 cm, 10 cm, 30 cm, and 60 cm. The eddy covariance (EC) system generates turbulent measurements of 3-D wind components (Campbell, CSAT 3) and of atmospheric concentrations of CO_2 and H_2O using an open path Infrared Gas Analyzer (LiCor LI-7500, IRGA). These scalars are measured at 20 Hz and are integrated over 30 minutes to generate surface fluxes according to CarboEurope-IP flux computation procedures (Béziat et al, 2009).

The LAI was also measured for these sites using a destructive method (Claverie 2012, Ferrant et al. 2014). At both flux sites, vegetation samples were collected along two transects crossing the field over the entire growing season until harvesting roughly once a month. Ten to twenty 1.5 m-long rows were collected on each sampling day. The organs of the collected plants were separated into green and yellow leaves, stems, flowers and fruits. The Plant Area Index (PAI) was defined as half the surfaces of all green organs, and the Leaf Area Index (LAI) was defined as half the surfaces of green leaves; it was measured by means of a LiCor planimeter (LI3100, LiCor, Lincoln, NE, USA).

Hydrol. Earth Syst. Sci. Discuss., doi:10.5194/hess-2016-661, 2017
Manuscript under review for journal Hydrol. Earth Syst. Sci.
Published: 10 January 2017

3 Methods

3.1 Numerical Experiments

We conducted two experiments to evaluate effects of the Formosat-2 LAI and land cover maps on the SURFEX-ISBA simulations. The simulated domain covers a 24x24 km area near Toulouse in southwestern France (Fig. 3). Simulations were carried out from 2006 to 2010. Our objective was to preserve the uniqueness of vegetation types within computation units to avoid mixing the LAI profiles of several crop types. A discretization of the domain with a regular grid based on cartographic coordinates as it is done by default via the SURFEX would require employing a grid resolution of at least 50 m to capture the spatial heterogeneity of the landscape (230,400 grid cells). The study area was thus discretized using an original approach: rather than using a regular grid, we used the land cover map to identify connected regions of pixels sharing a common PFT (using GDAL polygonize utility with 4-pixel connectedness). This discretization does not necessarily match actual crop fields because two adjacent fields with the same PFT are merged into one parcel. However, in general, a "numerical parcel" corresponds to a cultivated parcel. A parcel can also correspond to a non-cultivated area, such as a forest patch. These homogeneous parcels were determined for each year of the simulation period, as the land cover maps differ from one year to another mainly due to crop rotations. The parcel approach generates lower computation costs than the regular grid approach. The domain is composed of 12,500 to 14,500 parcels depending on the year considered, representing 84% to 91% of the total image area. The remaining surface corresponds to roads, lanes, rivers and strips of lawn between fields, which are not simulated in this study.

The first simulation (ECOCLIMAP) is the reference simulation. It simulates fluxes based on ECOCLIMAP-II vegetation parameters, including the climatological LAI and vegetation fraction (Sect. 2.1). ECOCLIMAP parameters are interpolated on parcel centroïds with interpolation functions included in the SURFEX-ISBA.

The second simulation (FORMOSAT) was carried out by prescribing the LAI using the monthly Formosat-2 LAI (Sect. 2.2.1) rather than the ECOCLIMAP-II LAI. Each parcel was also assigned a unique PFT obtained from the FORMOSAT land cover maps. We first aggregated the 34 classes of the original land cover maps to match the 12 standard PFTs of the SURFEX (Table 1). The other vegetation parameters were drawn from the ECOCLIMAP-II for the corresponding PFT.

3.2 Comparison methods

We extracted the outputs of both simulations from the Auradé and Lamasquère station parcels. We then calculated correlation coefficient (R^2) and Root-Mean Square Error (RMSE) values between monthly averages of the measured and simulated latent heat fluxes (LE, evapotranspiration). Then, we analyzed differences between both simulations for the entire modeling domain by calculating correlation coefficients between the monthly simulated evapotranspiration time series for each parcel. These correlation maps allow one to identify parcels where effects of using Formosat-2 data on the temporal evolution of evapotranspiration are more pronounced.

Hydrol. Earth Syst. Sci. Discuss., doi:10.5194/hess-2016-661, 2017
Manuscript under review for journal Hydrol. Earth Syst. Sci.
Published: 10 January 2017

Eventually, we aggregated the simulated LAI, evapotranspiration, drainage, runoff and Soil Water Index (SWI, Eq. (1), **Le Moigne 2012**) values of all of the parcels based on PFT values to analyze effects of the Formosat-2 products by vegetation type.

$$SWI = \frac{w - w_{wilt}}{w_{fc} - w_{wilt}} \quad (1)$$

where w is the volumetric soil water content, w_{wilt} is the volumetric soil water content at the wilting point and w_{fc} is the volumetric soil water content at field capacity.

4 Results

4.1 Local comparisons with in situ measurements

Our simulated evapotranspiration comparisons between eddy covariance measurements of the study sites in Auradé and Lamasquère show that using Formosat-2 data in the SURFEX simulation improves the correlation and RMSE of almost every year (Tables 2 and 3). The improvement is more significant when measurement fields are covered in sunflower or maize crops, i.e., summer crops. By contrast, the effects of Formosat-2 data are not as strong for wheat and rapeseed crops, i.e., winter crops.

To understand why these differences appear, we compared the time series of LAI and evapotranspiration for both sites for 2006 (Fig. 5 and 6). Silage maize was grown in Lamasquère in 2006. This crop is harvested before plant senescence; hence, the observed cycle is shorter than a typical maize cycle. Figure 5 shows that the LAI is more realistic when using Formosat-2 data rather than the ECOCLIMAP-II MODIS climatologic LAI. The FORMOSAT LAI phenological cycle is shorter and is in agreement with the LAI cycle observed in situ. LAI value increases due to crop growth and LAI value decline due to harvesting are well represented. By contrast, the ECOCLIMAP LAI is too high in the autumn and winter. This shows that for this specific location and vegetation type (C4 crop type), the ECOCLIMAP-II unmixing algorithm of MODIS LAI data does not allow one to capture the actual trajectory of LAI evolution. This may be attributable to (i) the unmixing algorithm itself, (ii) the temporal averaging method used to create the climatological LAI, and (iii) small woodland areas or strips of lawn between crops fields that cannot be resolved using MODIS, although they maintain moderate LAI values during the winter.

This better description of the LAI based on Formosat-2 leads to a better simulation of evapotranspiration timing (Fig. 6). In particular, the evapotranspiration peak is delayed by one month for summer crops (i.e., on Lamasquère) and thus fits the measurements better (Sect. 4.2 below). However, the Formosat-2 data do not match the actual amplitude of the evapotranspiration peak. This is most likely due to the lack of irrigation in the model given that the Lamasquère site was irrigated between June and August (147 mm). Adding the measured irrigation rates to the SAFRAN precipitation forcing improves this simulation with respect to LE measurements (not shown here).

Hydrol. Earth Syst. Sci. Discuss., doi:10.5194/hess-2016-661, 2017
Manuscript under review for journal Hydrol. Earth Syst. Sci.
Published: 10 January 2017

By contrast, differences in evapotranspiration levels are minor for the Auradé site, which was covered in wheat crops in 2006. LAI evolution patterns occurring during the crop growth period are similar. The main difference between both experiments occurs after the harvest period but does not lead to large differences in LE values (Sect. 4.2).

4.2 Spatial comparisons with the Formosat-2 image

We computed the correlation coefficient between the simulated evapotranspiration time series for both experiments for each parcel. Figure 7 illustrates the distribution of correlation coefficients grouped by land cover type. A small correlation value denotes that the evapotranspiration time series are not in phase. Evapotranspiration patterns are not heavily modified outside of the crop fields (Fig. 7a), generating a correlation coefficient of almost 1 and low levels of value dispersion. From the crop areas, two populations can be identified: winter and summer crops. The temporal evolution of winter crop evapotranspiration (mostly wheat, C3) is not heavily modified (Fig. 7b). However, the effect is much more significant for summer crops (mostly maize (C4), sunflower (C3) and soy (C3) plants), generating a median correlation coefficient that is lower than that of wheat and a considerable degree of value dispersion depending on the year (Fig. 7c and 7d).

Local results suggest that the ECOCLIMAP LAI forcing does not allow for a correct representation of the evapotranspiration fluxes of summer crops over the entire domain because it does not capture their phenology with sufficient precision, especially in regard to the temporal extent of the cycle. Replacing the C3 and C4 classes of the ECOCLIMAP (based on the plant photosynthesis mechanism) with summer and winter crops classes, even when using a climatologic LAI, may increase the precision of simulated evapotranspiration patterns for these types of crops. The identified dependence on the year may be due to agricultural practices such as sowing or harvesting dates, which are related to climatic conditions of a given year. The MODIS climatologic LAI included in ECOCLIMAP-II cannot simulate interannual variability like Formosat-2. It is thus unable to capture effects of these practices on vegetation phenology, thus producing significant differences from the actual LAI cycle.

To further understand effects on hydrometeorological processes, we compared the monthly differences of both experiments on LAI and evapotranspiration (LE) dynamics. The results were aggregated by averaging each variable of all of the C4 crop fields (maize and sorghum) for 2008 (Fig. 8a). We also compared daily Soil Water Index (SWI, Fig. 8b), drainage (DRAIN) and runoff (Fig. 8c) differences. As was done for the previous point-scale analysis (Sect. 4.1), the difference in LE denotes the delay in the evapotranspiration peak with a negative difference occurring during the spring (ECOCLIMAP is higher than FORMOSAT) and with a peak occurring during the summer (Fig. 8a). It is strongly correlated with the difference in LAI as well. The lower LAI level occurring during the spring in the FORMOSAT experiment induces a lower transpiration level because the evaporative surfaces of each plant are restricted, thus enhancing their capacity for stomatal resistance. As a result, the SWI remains higher than that of the ECOCLIMAP simulation until the summer (Fig 8b). A higher SWI recorded during the summer denotes that more water remains available for evaporation from the soil, thus rendering the LE is higher during this period according to FORMOSAT experimental results. This explains why the LE difference is positive during the summer even when there is almost no difference in LAI values. In the ISBA-SURFEX, drainage only occurs when the SWI

Hydrol. Earth Syst. Sci. Discuss., doi:10.5194/hess-2016-661, 2017
Manuscript under review for journal Hydrol. Earth Syst. Sci.
Published: 10 January 2017

is higher than 1 (Le Moigne, 2012), and so an increase in the SWI during the spring causes an increase in the drainage volume (Fig. 8c), which can be significant over the year (Table 4), averaging at approximately 4% of annual precipitation and at up to 8% for sunflower and wheat crop fields. Runoff is also affected by differences in the SWI (table 5) but in smaller proportions. Indeed, the function used in both of our experiments to simulate runoff is based on the premise that even when the SWI is lower than 1, rain can saturate part of a pixel's upper soil layer, thus generating runoff in the pixel. This dripping section of a pixel increases with soil moisture. This is not the case for drainage patterns, which require a saturation of the entire soil root layer to occur. Thus, a higher SWI, even if it remains below a value of 1, suggests that a larger part of a pixel is dripping, thus causing runoff levels to be higher in the FORMOSAT experiment (Fig 8c). However, irrigation concerns continue to be the main limitation of our study given that roughly 13% of the fields in our domain are irrigated. Incorporating irrigation rules similar to those of the MAELIA platform (Therond & al., 2014**)** could thus affect evapotranspiration values and consequently SWI and drainage values.

5 Conclusion

The use of high spatial resolution and high revisit frequency Formosat-2 data rather than standard ECOCLIMAP-II vegetation parameters was found to improve the representation of the vegetation phenology of the SURFEX for a cultivated area characteristic of southwestern France. Local comparisons with in situ observations show that this in turn improves monthly evapotranspiration simulations. This finding is particularly true for summer crops, whereas the impact is less significant for winter crops and is even less significant outside of crop areas. From our spatial comparisons, we suggest that our local scale results are likely transposable across the whole domain.

For crop growing areas, the Formosat-2 LAI is lower than that of ECOCLIMAP-II before crops grow, and thus, the Soil Water Index (SWI) remains higher during the crop growing season. As a result, drainage and runoff levels are higher. The SWI also decreases later in the summer, making more water available for evaporation from the soil in the summer. This phenomenon generates a significant increase in evapotranspiration during the summer for summer crops when Formosat-2 products are used. Employing the ECOCLIMAP-II classification with a summer crop class may constitute a first step to ameliorating ISBA-SURFEX model realism when it is applied to agricultural areas even with a climatologic LAI.

More generally, we showed that high-resolution land cover maps and LAI time series allow one to take into account effects of the actual vegetative cycle of each parcel in an operational hydrometeorological model. These remote sensing products capture complex anthropogenic effects on land surface properties (e.g., sowing and harvest dates and fertilizer inputs). In the present study, Formosat-2 data were limited to a 24 km by 24 km area whereas water management agencies typically manage river basins at a regional scale (above 10^4 km²). Sentinel-2A already images the Earth' land area at a similar radiometric spatial resolution over a 10-day revisit period. The optimal revisit period of 5 days should be achieved in the next few months after the launch of Sentinel-2B. Our study shows that Sentinel-2 observations will soon allow us to improve the monitoring of water resources in large anthropized river basins. Scalable algorithms for crop type mapping and LAI

retrieval are now available (Li & al., 2015; Inglada & al., 2015), allowing for the processing of large areas. While the computation costs of the hydrometeorological model at this spatial resolution may be an issue, the SURFEX land surface model can run in a parallel mode using the Message Passing Interface protocol. Therefore, the focus of our future studies will be to upscale this methodology to the Garonne River Basin using Landsat and SPOT-4/5 Take 5 data (Hagolle & al., 2015) to evaluate the impact of these data on river discharge and groundwater recharge at the water resource management scale.

Additional work must also be conducted to explicitly represent irrigation in the model. The approach presented in this paper enables one to better match the timing of evapotranspiration over irrigated areas. However, it fails to represent its actual amplitude, as there is no parameterization for water uptake from an aquifer or from surface water. Ongoing developments will focus on the implementation of parsimonious rule-based irrigation parameterizations in the ISBA-SURFEX (Martin & al., 2016). These developments will directly benefit from the high-resolution application of the ISBA-SURFEX presented in this paper, as irrigation rules are partly constrained by land cover type (Therond & al., 2014).

The supplements related to this article are available online at: http://tully.ups-tlse.fr/simon/surfex-configuration-files

Code and data availability

The version of SURFEX used in this study is the v7.3. The code is available here: http://www.umr-cnrm.fr/surfex//data/BROWSER/out_doc73/index.html.

For the LAI data or land cover maps, please ask to the corresponding author.

Author contribution:

J. Etchanchu formatted the data, performed the simulation, analyzed the results and wrote most of the current paper.

V. Rivalland and S. Gascoin helped at designing the experiments, processing the data and analyzing the results.

J. Cros provided the tools to process the remote sensing data.

A. Brut wrote the section 2.2.3 about the instrumentation of the two stations.

All the authors revised the paper.

Acknowledgments:

This study was conducted as part of the REGARD project entitled « Modélisation des REssources en eau sur le basin de la GAronne, interaction entre les composantes naturelles et anthropiques et apport de la téléDétection » (http://www.cnrm-

game-meteo.fr/spip.php?article809) funded by the French "Sciences and Technologies for Aeronautics and Space" Foundation (http://www.fondationstae.net). We thank Mathieu Coustau for his work, which formed the basis of our paper.

References

Allen, R.G., Pereira, L.S., Raes, D., Smith, M.: Crop evapotranspiration — guidelines for computing crop water requirements, FAO Irrigation and drainage paper 56, Food and Agriculture Organization, Rome, 1998.

Béziat, P., Ceschia, E., Dedieu, G.: Carbon balance of a three crop succession over two cropland sites in South West France, Agr. Forest Meteorol., 149 (10), 1628–1645, doi: 10.1016/j.agrformet.2009.05.004, 2009.

Boussetta, S., Balsamo, G., Beljaars, A., Kral, T. and Jarlan, L.: Impact of a satellite-derived leaf area index monthly climatology in a global numerical weather prediction model, Int. J. Remote Sens., Special Issue, Third International Symposium on Recent Advances in Quantitative Remote Sensing, 34, 9-10, 3520-3542, doi: 10.1080/01431161.2012.716543, 2013.

Claverie, M.: Estimation spatialisée de la biomasse et des besoins en eau des cultures à l'aide de données satellitales à hautes résolutions spatiale et temporelle : application aux agrosystèmes du sud-ouest de la France, Ph.D. thesis, Université Toulouse III – Paul Sabatier, 2012.

Dejoux, J.F., Dedieu, G., Hagolle, O., Ducrot, D., Menaut, J.C., Ceschia, E., Baup, F., Demarez, V., Marais-Sicre, C., Kadiri, M., & al. : Kalideos OSR MiPy : un observatoire pour la recherche et la demonstration des applications de la télédétection à la gestion des territoires, Revue Française de Photogrammétrie et de Télédétection, Société Française de Photogrammétrie et de Télédétection, 17-30, 2012.

Ducrot, D. : Méthodes d'analyse et d'interprétation d'images de télédétection multi-sources -Extraction de caractéristiques du paysage, « Habilitation à Diriger des Recherches » thesis, INP Toulouse, 2005.

Ducrot, D., Gouaux, P. : Paysage et Télédétection dans les processus écologiques : Caractérisation des paysages par télédétection, source d'indicateurs de leur fonctionnement, JET Journées d'Ecologie Fonctionnelle, Biarritz, France, 2007.

Ducrot, D., Ceshia, E., Marais-Sicre, C.: Détection des changements de l'occupation du sol à partir d'images de télédétection multi-temporelles, « Changement de paysage » conference, Tunis, 2009.

FAO/IIASA/ISRIC/ISS-CAS/JRC: Harmonized World Soil Database (version 1.2), FAO, Rome, Italy and IIASA, Laxenburg, Austria, 2012.

Faroux, S., Kaptué Tchuenté, A.T., Roujean, J.-L., Masson, V., Martin, E., Le Moigne, P.: ECOCLIMAP-II/Europe: a twofold database of ecosystems and surface parameters at 1km resolution based on satellite information for use in land surface, meteorological and climate models, Geoscientific Model Development, 6, 563-582, doi: 10.5194/gmd-6-563-2013, 2013.

Ferrant, S., Gascoin, S., Veloso, A., Salmon-Monviola, J., Claverie, M., Rivalland, V., Dedieu, G., Demarez, V., Ceschia, E., Probst, J.L., Durand, P., Bustillo, V.: Agro-hydrology and multi-temporal high-resolution remote sensing : toward an explicit spatial processes calibration, Hydrol. Earth Syst. Sc., 18, 5219-5237, doi: 10.5194/hess-18-5219-2014, 2014.

Ferrant, S., Bustillo, V., Burel, E. Salmon-Monviolla, J., Claverie, M., Jarosz, N., Yin, T., Rivalland, V., Dedieu, G., Demarez, V., Ceschia, E., Probst, A., Al-Bitar, A., Kerr, Y., Probst, J-L., Durand, P., Gascoin, S.: Extracting soil water holding capacity parameters of a distributed agro-hydrological model from high resolution optical satellite observation series, Remote Sensing, 8(2), 154, doi:10.3390/rs8020154, 2016.

Foley, J.A., DeFries, R., Asner, G.P., Barford, C., Bonan, G., Carpenter, S.R., Chapin, F.S., Coe, M.T., Daily, G.C., Gibbs, H.K., Helkowski, J.H., Holloway, T., Howard, E.A., Kucharik, C.J., Monfreda, C., Patz, J.A., Prentice, I.C., Ramankutty, N., Snyder, P.K.: Global consequences of land use, Science, 309(5734), 570-574, doi: 10.1126/science.1111772, 2005.

Ford, T.W., Quiring, S.M.: Influence of MODIS-derived dynamic vegetation on VIC-simulated soil moisture in Oklahoma, J. Hydrometeorol., 14(6), 1910–1921, doi: 10.1175/JHM-D-13-037.1, 2013.

Habets F., Boone, A., Champeaux, J.L., Etchevers, P., Franchistéguy, L., Leblois, E., Ledoux, E., Le Moigne, P., Martin, E., Morel, S., Noilhan, J., Quintana Segui, P., Rousset-Regimbeau, F., Viennot, P.: The SAFRAN-ISBA-MODCOU hydrometeorological model applied over France, J. Geophys. Res., 113, D06113 (2008) 18, doi: 10.1029/2007JD008548, 2008.

Hagolle, O., Dedieu, G., Mougenot, B., Debaeker, V.,Duchemin, B., Meygret, A.: Correction of aerosol effects on multi-temporal images acquired with constant viewing angles: application to Formoat-2 images, Remote Sens. Environ., 112, 1689-1701, doi:10.1016/j.rse.2007.08.016, 2008.

Hagolle, O., Huc, M., Pascual, D. V., Dedieu, G.: A multi-temporal method for cloud detection, applied to FORMOSAT-2, VENuS, LANDSAT and SENTINEL-2 images, Remote Sens. Environ., 114, 1747-1755, doi:10.1016/j.rse.2010.03.002, 2010.

Hagolle, O., Sylvander, S., Huc, M., Claverie, M., Clesse, D., Dechoz, C., Lonjou, V., Poulain, V.: SPOT-4 (Take 5): simulation of Sentinel-2 time series on 45 large sites, Remote Sensing, 7(9), 12242-12264, doi: 10.3390/rs70912242, 2015.

Inglada, J., Arias, M., Tardy, B., Hagolle, O., Valero, S., Morin, D., Dedieu, G., Sepulcre, G., Bontemps, S., Defourny, P., Koetz, B.: Assessment of an operational system for crop type map production using high temporal and spatial resolution satellite optical imagery, Remote Sensing, 7(9), 12356-12379, doi: 10.3390/rs70912356, 2015.

Jarlan, L., Balsamo, G., Lafont, S., Beljaars, A., Calvet, J.C., Mougin, E.: Analysis of leaf area index in the ECMWF land surface model and impact on latent heat and carbon fluxes : application to West Africa, J. Geophys. Res., 113(D24), doi: 10.1029/2007JD009370, 2008.

Le Moigne, P., Surfex scientific documentation, 2012.

Li, W., Weiss, M., Waldner, F., Defourny, P., Demarez, V., Morin, D., Hagolle, O., Baret, F.: A Generic algorithm to estimate LAI, FAPAR and FCOVER variables from SPOT4_HRVIR and Landsat sensors: evaluation of the consistency and comparison with ground measurements, Remote Sensing, 7(11), 15494-15516, doi: 10.3390/rs71115494, 2015.

Martin, E., Gascoin, S., Grusson, Y., Murgue, C., Bardeau, M., Anctil, F., Ferrant, S., Lardy, R., et al.: On the use of hydrological models and satellite data to study the water budget of river basins affected by human activities: examples from the Garonne basin of France, Surv. Geophys., 37(2), 223-247, doi: 10.1007/s10712-016-9366-2, 2016

Masson, V., Champeaux, J.L., Chauvin, F., Meriguet, C., Lacaze, R.: A global database of land surface parameters at 1-km resolution in meteorological and climate models, J. Climate, 16(9), 1261-1282, doi:10.1175/1520-0442-16.9.1261, 2003.

Masson, V., Le Moigne, P., Martin, E., Faroux, S., Alias, A., Alkama, R., Belamari, S., Barbu, A., Boone, A., Bouyssel, F., Brousseau, P., Brun, E., Calvet, J.C., Carrer, D., Decharme, B., Delire, C., Donier, S., Essaouini, K., Gibelin, A.L., Giordani, H., Habets, F., Jidane, M., Kerdraon, G., Kourzeneva, E., Lafaysse, M., Lafont, S., Lebeaupin Brossier, C., Lemonsu, A., Mahfouf, J.F., Marguinaud, P., Mokhtari, M., Morin, S., Pigeon, G., Salgado, R., Seity, Y., Taillefer, F., Tanguy, G., Tulet, P., Vincendon, B., Vionnet, V., Voldoire, A.: The SURFEX v7.2 land and ocean surface platform for coupled or offline simulation of earth surface variables and fluxes, Geoscientific Model Development, 6, 929-960, doi:10.5194/gmd-6-929-2013, 2013.

Maurer, E.P., Wood, A.W., Adam, J.C., Lettenmaier, D.P.: A long term hydrologically based dataset of land surface fluxes and states for the conterminous United States, J. Climate, 15, 3237-3251, doi: 10.1175/1520-0442(2002)015<3237:ALTHBD>2.0.CO;2, 2002.

Nagler, P.L., Glenn, E.P., Nguyen, U., Scott, R.L., Doddy, T.: Estimating Riparian and Agricultural Actual evapotranspiration by reference evapotranspiration and MODIS Enhanced Vegetation Index, Remote Sensing, 5(8), 3849-3871, doi: 10.3390/rs5083849, 2013.

Oleson, K.W., Niu, G.Y., Yang, Z.L., Lawrence, D.M., Thorton, P.E., Lawrence, P.J., Stöckli, R., Dickinson, R.E., Bonan, G.B., Levis, S., Dai, A., Qian, T.: Improvements to the Community Land Model and their impact on the hydrological cycle, J. Geophys. Res., 113, G01021, doi: 10.1029/2007JG000563, 2008.

Pauwels, V.R.N., Verhoest, N.E.C., De Lannoy, G.J.M., Guissard, V., Lucau, C., Defourny, P.: Optimization of a coupled hydrology-crop growth model trough the assimilation of observed soil moisture and leaf area index values using an ensemble Kalman filter, Water Resour. Res., 43, W04421, doi: 10.1029/2006WR004942, 2007.

Quintana-Segui, P., Le Moigne, P., Durand, Y., Martin, E., Habets, F., Baillon, M., Canellas, C., Franchisteguy, L., Morel, S.: Analysis of near-surface atmospheric variables: validation of the SAFRAN analysis over France, J. Appl. Meteorol. Clim., 47, 92-107, doi: 10.1175/2007JAMC1636.1, 2007.

Tang, Q., Vivoni, E.R., Muñoz-Arriola, F., Lettenmaier D.P.: Predictability of evapotranspiration patterns using remotely sensed vegetation dynamics during the North American Monsoon, J. Hydrometeorol., 13, 103–121, doi: 10.1175/JHM-D-11-032.1, 2012.

Tesemma, Z. K., Wei, Y., Peel, M. C., Western, A. W.: The effect of year-to-year variability of leaf area index on Variable Infiltration Capacity model performance and simulation of runoff, Adv. Water Resour., 83, 310-322, doi: 10.1016/j.advwatres.2015.07.002, 2015.

Therond, O., Sibertin-Blanc, C., Lardy, R., Gaudou, B., Balestrat, M., Hong, Y., Louail, T., Nguyen, V.B., Panzoli, D., Sanchez-Perez, J.M., Sauvage, S., Taillandier, P., Vavasseur, M., Mazzega, P.: Integrated modelling of social-ecological systems: The MAELIA high-resolution multi-agent platformto deal with water scarcity problems, International Environmental Modelling and Software Society (iEMSs), 7th International Congress on Environmental Modelling and Software, San Diego, CA, USA, 2014.

Trezza, R., Allen, R.G., Tasumi, M.: Estimation of actual evapotranspiration along the Middle Rio Grande of New Mexico using MODIS and Landsat imagery with the METRIC model, Remote Sensing, 5, 5397-5423, doi: 10.3390/rs5105397, 2013.

Van den Hurk, B.J.J.M., Viterbo, P., Los, S.O.: Impact of leaf area index seasonality on the annual land surface evaporation in a global circulation model, J. Geophys. Res., 108, D64191, doi: 10.1029/2002JD002846, 2003.

Veloso, A., Demarez, V., Ceschia, E.: Retrieving crops Green Area Index from high resolution multisensor remote sensing data, Proceedings of Sentinel-2 Preparatory Symposium, 2012.

Verseghy, D.L., McFarlane, N.A., Lazare, M.: CLASS – A Canadian land surface scheme for GCMS, II. Vegetation model and coupled runs, Int. J. Climatol., 13, 347-370, doi: 10.1002/joc.3370130402, 1993.

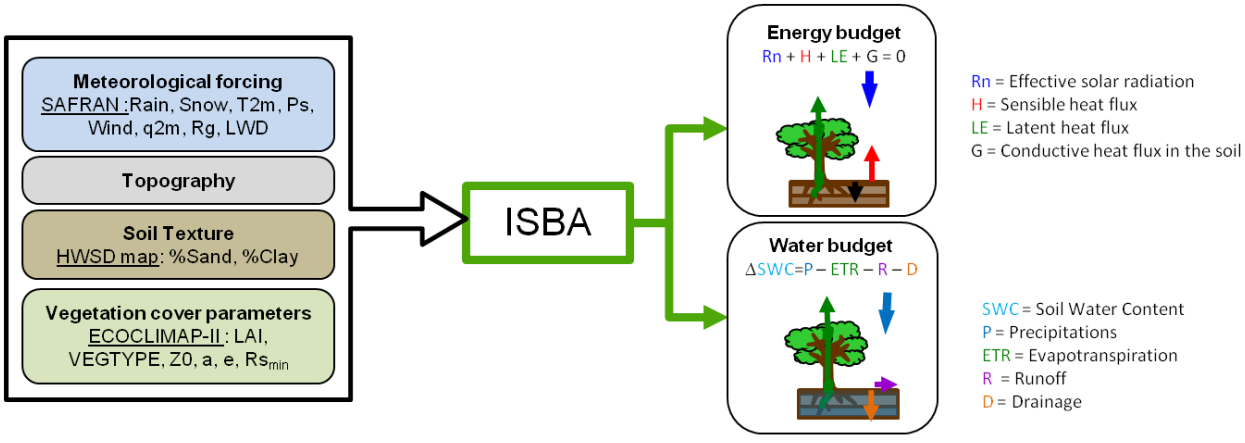

Figure 1: Schematic flowchart of ISBA inputs and outputs.

Hydrol. Earth Syst. Sci. Discuss., doi:10.5194/hess-2016-661, 2017
Manuscript under review for journal Hydrol. Earth Syst. Sci.
Published: 10 January 2017

Hydrology and Earth System Sciences
Discussions

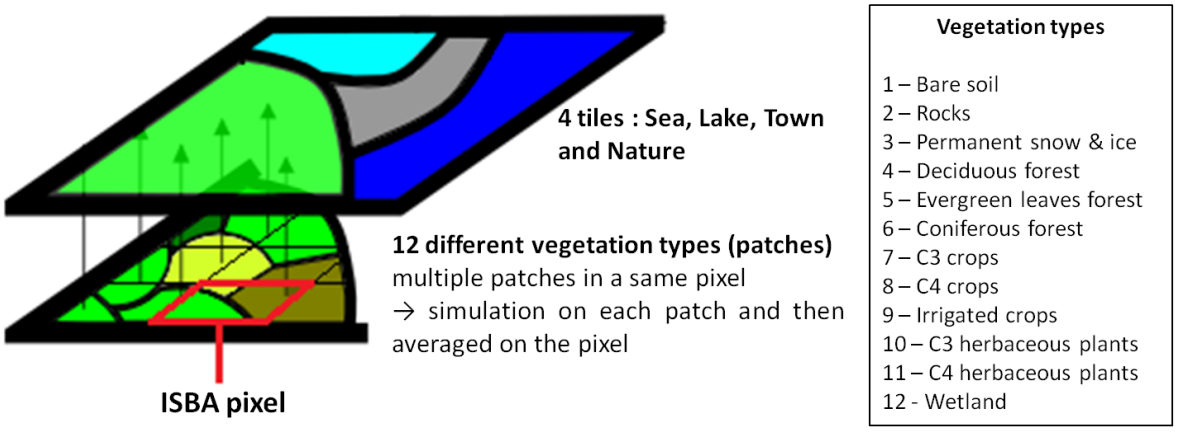

Figure 2: ISBA patch simulation principles.

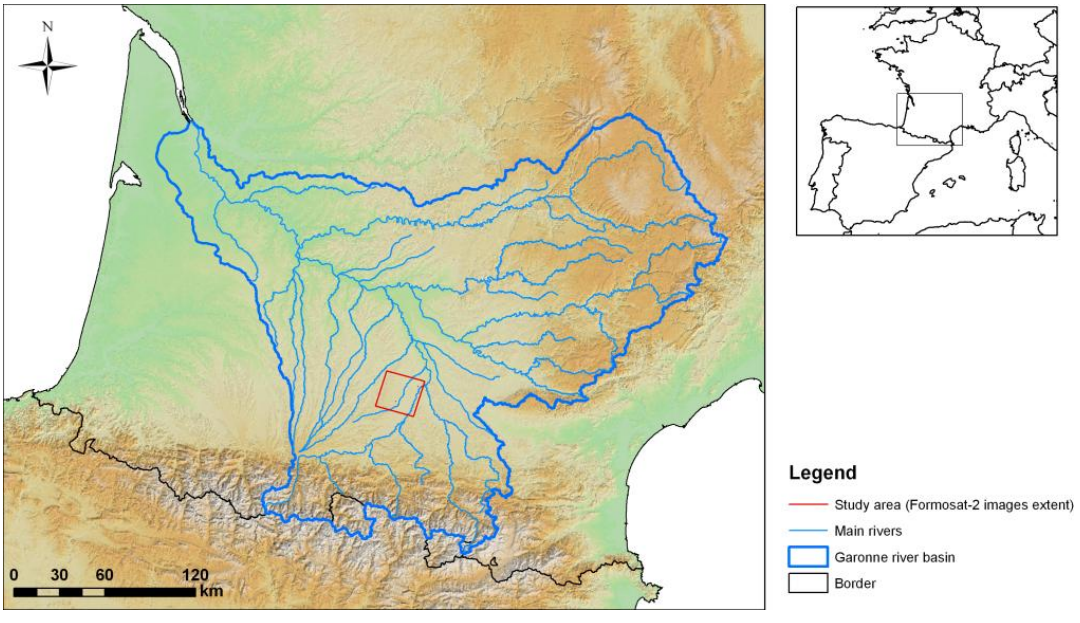

Figure 3: Study area location (red)

Hydrol. Earth Syst. Sci. Discuss., doi:10.5194/hess-2016-661, 2017
Manuscript under review for journal Hydrol. Earth Syst. Sci.
Published: 10 January 2017

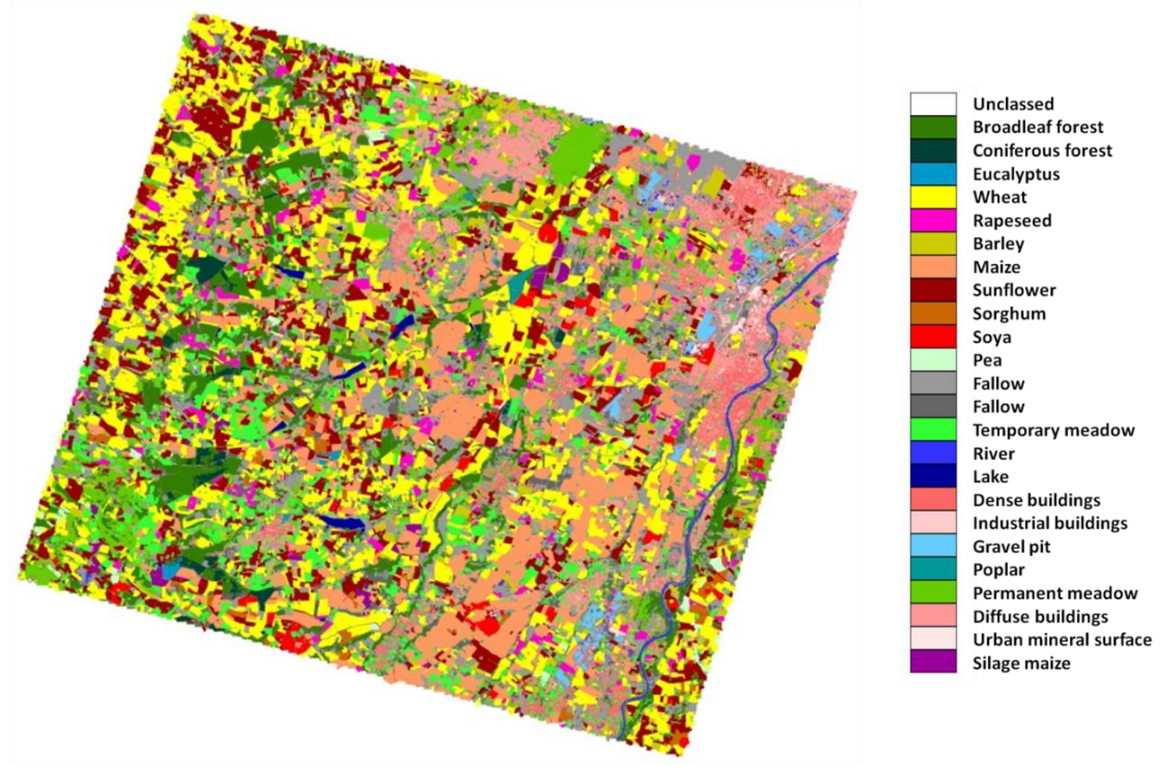

Figure 4: Land cover map for 2006

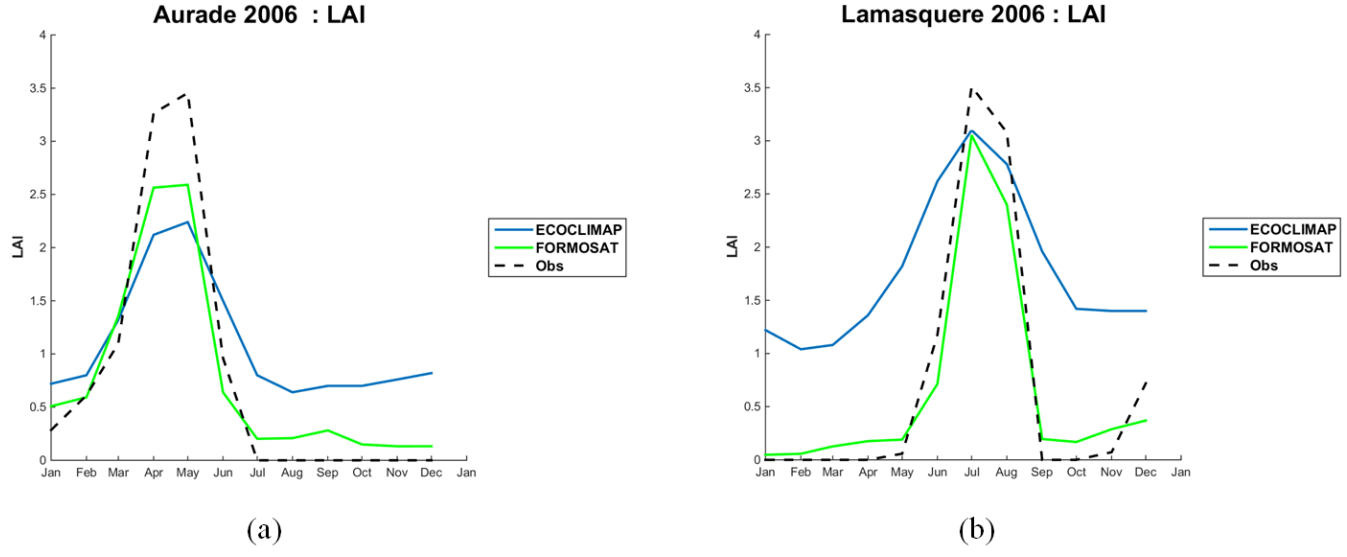

Figure 5: LAI time series for Auradé (a) and Lamasquère (b) for 2006

Hydrol. Earth Syst. Sci. Discuss., doi:10.5194/hess-2016-661, 2017
Manuscript under review for journal Hydrol. Earth Syst. Sci.
Published: 10 January 2017

Hydrology and Earth System Sciences
Discussions
Open Access
EGU

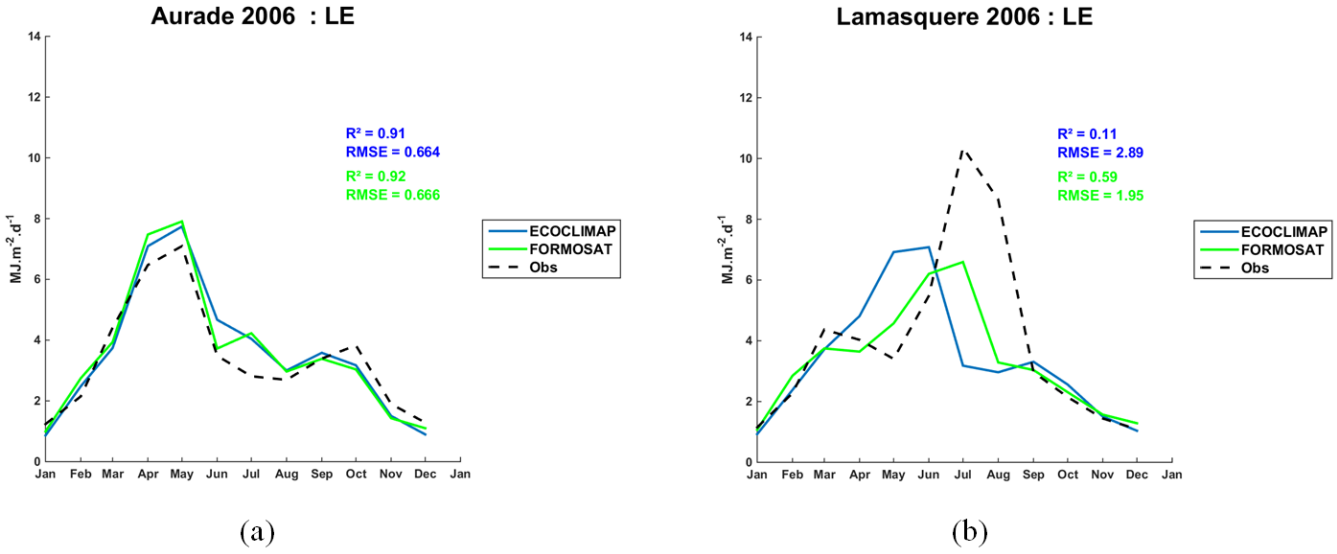

Figure 6: Evapotranspiration time series for Auradé (a) and Lamasquère (b) for 2006

Hydrol. Earth Syst. Sci. Discuss., doi:10.5194/hess-2016-661, 2017
Manuscript under review for journal Hydrol. Earth Syst. Sci.
Published: 10 January 2017

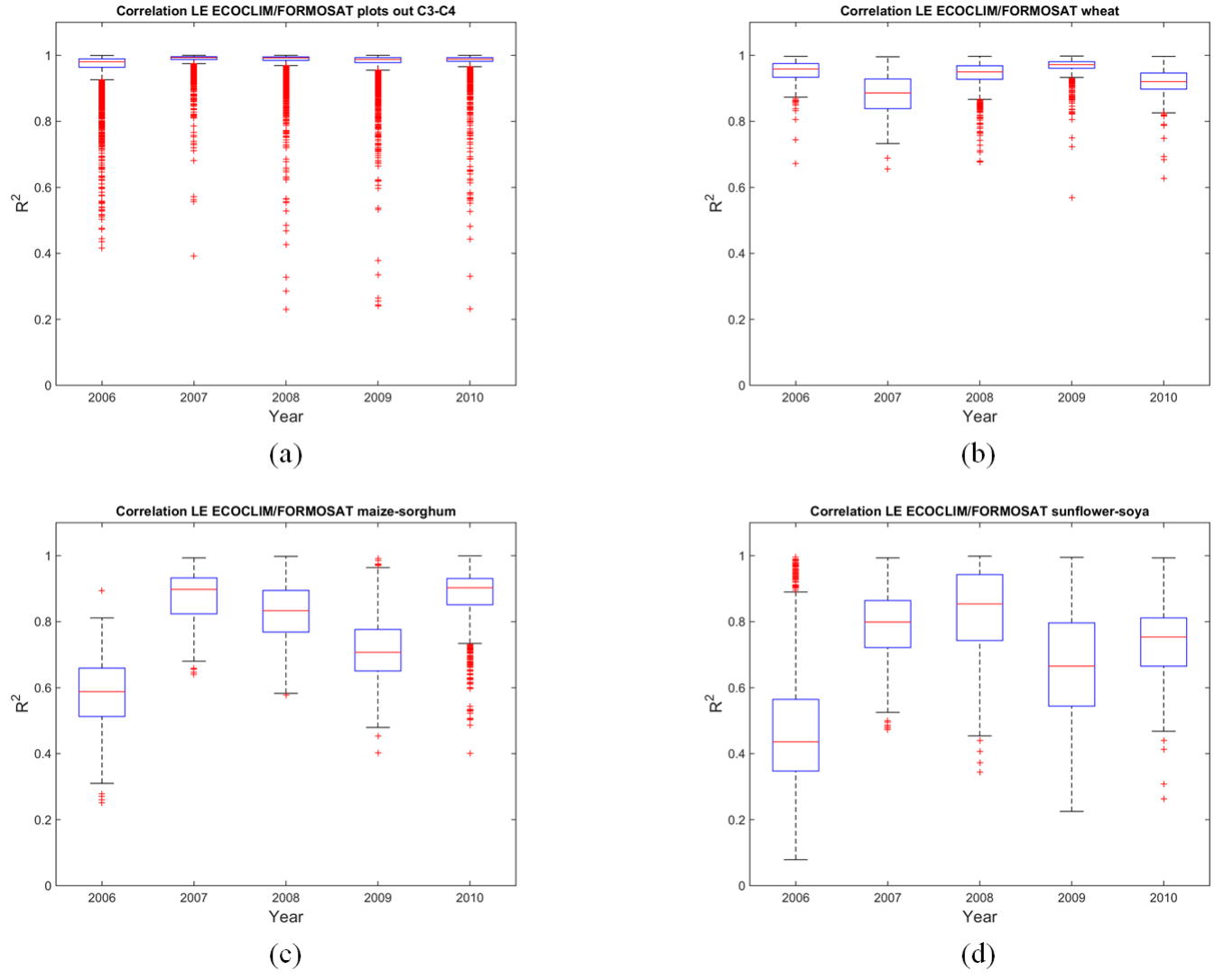

Figure 7: Correlations between the evapotranspiration time series of the two experiments on: (a) uncultivated plots; (b) wheat crops; (c) C4 crops (maize and sorghum); and (d) sunflower and soy crops. The boxplots show the medians in red. Edges of each box represent quartiles whereas whiskers represent extreme values not considered as outliers (red dots for the outliers).

Hydrol. Earth Syst. Sci. Discuss., doi:10.5194/hess-2016-661, 2017
Manuscript under review for journal Hydrol. Earth Syst. Sci.
Published: 10 January 2017

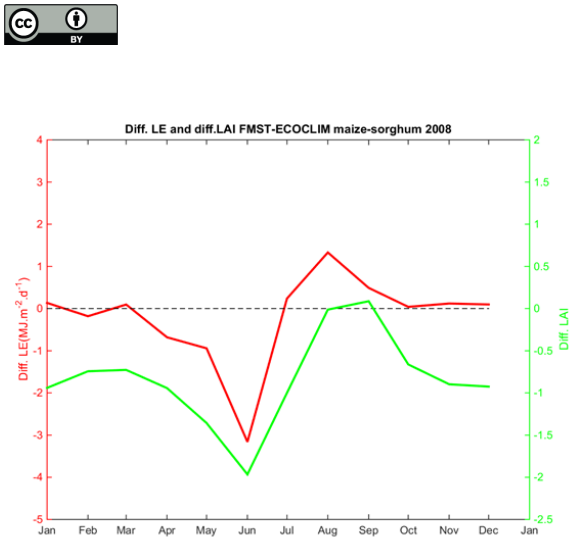

(a)

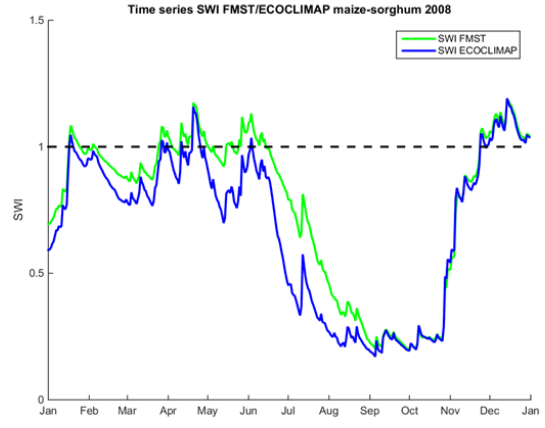

(b)

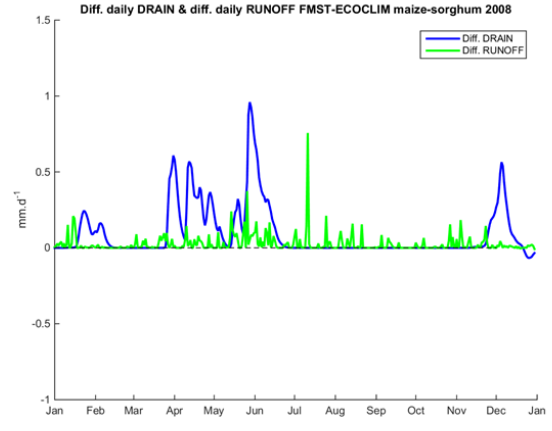

(c)

Hydrol. Earth Syst. Sci. Discuss., doi:10.5194/hess-2016-661, 2017
Manuscript under review for journal Hydrol. Earth Syst. Sci.
Published: 10 January 2017

Hydrology and Earth System Sciences
Open Access
Discussions

Figure 8: (a) Differences in LAI (green) and evapotranspiration (red) between the two experiments (FORMOSAT-ECOCLIMAP) ; (b) Time series of Soil Water Index; (c) Differences in drainage (blue) and runoff (green) values; Averaged across C4 crops for 2008

5

Hydrol. Earth Syst. Sci. Discuss., doi:10.5194/hess-2016-661, 2017
Manuscript under review for journal Hydrol. Earth Syst. Sci.
Published: 10 January 2017

Formosat-2 cover map class	SURFEX class
16. Bare soil	1. Bare soil
4. Urban area 33. Gravel pit 41. Dense buildings 42. Diffuse buildings 43. Industrial buildings 44. Urban mineral surface	2. Rocks
-	3. Permanent snow and ice
231. Mixed broadleaf forest 2311. Poplar 2312. Eucalyptus	4. Deciduous forest
-	5. Evergreen forest
232. Mixed coniferous forest	6. Coniferous forest
15. Dual crops 121. Wheat 122. Barley 123. Rapeseed 132. Sunflower 134. Soya 135. Hemp 141. Protein plants 142. Spring barley 1321. Late sunflower 1411. Pea	7. C3 crops
131. Maize 133. Sorghum 1311. Non-irrigated maize 1312. Silage maize	8. C4 crops
-	9. Irrigated crops
22. & 112. Fallow 111. Meadow 1111. Temporary meadow 1112. Permanent meadow	10. C3 herbaceous plants
-	11. C4 herbaceous plants
31. River 32. Lake	12. Wetland

Table 1: Aggregation rules of Formosat-2 cover maps by SURFEX vegetation type

Hydrol. Earth Syst. Sci. Discuss., doi:10.5194/hess-2016-661, 2017
Manuscript under review for journal Hydrol. Earth Syst. Sci.
Published: 10 January 2017

Hydrology and Earth System Sciences
Discussions

Year	Crop type	R^2 ECOCLIMAP	R^2 FORMOSAT	RMSE ECOCLIMAP	RMSE FORMOSAT
2006	Wheat	0,91	0,92 =	0,67	0,66 =
2007	Sunflower	0,67	0,90 +++	1,72	0,98 +++
2008	Wheat	0,80	0,90 +	2,68	1,69 +++
2009	Rapeseed	0,96	0,96 =	0,59	0,64 =
2010	Wheat	0,89	0,98 +	1,72	1,65 =

Table 2: Correlation coefficient and Root-Mean Square Error of evapotranspiration for the Auradé site

Year	Crop type	R^2 ECOCLIMAP	R^2 FORMOSAT	RMSE ECOCLIMAP	RMSE FORMOSAT
2006	Maize	0,11	0,59 +++	2,89	1,95 +++
2007	Wheat	0,77	0,95 ++	1,84	1,29 ++
2008	Maize	0,51	0,79 +++	2,35	1,63 +++
2009	Wheat	0,91	0,94 =	1,7	1,16 ++
2010	Maize	0,52	0,68 ++	2,1	1,69 ++

Table 3: Correlation coefficient and Root-Mean Square Error of evapotranspiration for the Lamasquère site

Vegetation type	2006	2007	2008	2009	2010	Interannual mean
Outside the crops	+15 (+2.9%)	+16 (+2.3%)	+41 (+5.3%)	+20 (+3.1%)	+30 (+4.7%)	+24 (+3.7%)
Wheat	-3 (-0.6%)	-1 (-0.2%)	+61 (+8.0%)	+15 (+2.3%)	+20 (+3.1%)	+18 (+2.8%)
Sunflower/soya	+5 (+0.9%)	+54 (+7.9%)	+47 (+6.1%)	+30 (+4.7%)	+48 (+7.5%)	+37 (+5.7%)
Maize/sorghum	+4 (+0.7%)	+35 (+5.2%)	+35 (+4.6%)	+18 (+2.8%)	+32 (+5.0%)	+25 (+3.8%)

Table 4: Differences between FORMOSAT and ECOCLIMAP experiments on the annual drainage level in mm.yr^{-1} and the corresponding fraction of annual precipitations in % (FORMOSAT-ECOCLIMAP).

Hydrol. Earth Syst. Sci. Discuss., doi:10.5194/hess-2016-661, 2017
Manuscript under review for journal Hydrol. Earth Syst. Sci.
Published: 10 January 2017

Hydrology and Earth System Sciences
Open Access
Discussions

Vegetation type	2006	2007	2008	2009	2010	Interannual mean
Outside the crops	+3 (+0.6%)	+4 (+0.6%)	+7 (+0.9%)	+4 (+0.6%)	+4 (+0.7%)	**+4 (+0.6%)**
Wheat	+1 (+0.2%)	+5 (+0.7%)	+17 (+2.3%)	+7 (+1.1%)	+4 (+0.6%)	**+7 (+1%)**
Sunflower/soya	+7 (+1.4%)	+13 (+1.9%)	+10 (+1.4%)	+11 (+1.7%)	+13 (+2.0%)	**+11 (+1.7%)**
Maize/sorghum	+6 (+1.1%)	+9 (+1.3%)	+10 (+1.3%)	+9 (+1.4%)	+9 (+1.4%)	**+9 (+1.3%)**

Table 5: Differences between FORMOSAT and ECOCLIMAP experiments on annual runoff in mm.yr^{-1} and the corresponding fraction of annual precipitations in % (FORMOSAT-ECOCLIMAP).